# Conditional Control of Donor Nuclear Spins in Silicon Using Stark Shifts

Gary Wolfowicz,[1,2,*] Matias Urdampilleta,[1] Mike L. W. Thewalt,[3] Helge Riemann,[4] Nikolai V. Abrosimov,[4] Peter Becker,[5] Hans-Joachim Pohl,[6] and John J. L. Morton[1,7,†]

[1]*London Centre for Nanotechnology, University College London, London WC1H 0AH, United Kingdom*
[2]*Department of Materials, Oxford University, Oxford OX1 3PH, United Kingdom*
[3]*Department of Physics, Simon Fraser University, Burnaby, British Columbia V5A 1S6, Canada*
[4]*Institute for Crystal Growth, Max-Born Strasse 2, D-12489 Berlin, Germany*
[5]*Physikalisch-Technische Bundesanstalt, D-38116 Braunschweig, Germany*
[6]*Vitcon Projectconsult GmbH, 07745 Jena, Germany*
[7]*Department of Electronic & Electrical Engineering, University College London, London WC1E 7JE, United Kingdom*

(Received 29 May 2014; published 6 October 2014)

Electric fields can be used to tune donor spins in silicon using the Stark shift, whereby the donor electron wave function is displaced by an electric field, modifying the hyperfine coupling between the electron spin and the donor nuclear spin. We present a technique based on dynamic decoupling of the electron spin to accurately determine the Stark shift, and illustrate this using antimony donors in isotopically purified silicon-28. We then demonstrate two different methods to use a dc electric field combined with an applied resonant radio-frequency (rf) field to conditionally control donor nuclear spins. The first method combines an electric-field induced conditional phase gate with standard rf pulses, and the second one simply detunes the spins off resonance. Finally, we consider different strategies to reduce the effect of electric field inhomogeneities and obtain above 90% process fidelities.

DOI: 10.1103/PhysRevLett.113.157601 PACS numbers: 76.30.-v, 03.67.-a, 71.55.-i, 76.70.Dx

The manipulation of donor spins in silicon is mainly realized by the application of resonant ac magnetic fields. These can be used to globally control a large ensemble of spins with high fidelity [1], and also to control a single spin [2,3]. However, applying local ac magnetic fields to donors in an interacting array is practically challenging, especially considering the number of high frequency, high power microwave lines in a mature device. For such reasons, the majority of scalable quantum computing architectures based on donors in silicon [4–6], combine globally applied ac magnetic fields with the ability to electrically tune the donor spin, via the Stark effect which primarily modulates the hyperfine interaction between the electron and nuclear spin.

The Stark effect arises from a perturbation of the electron wave function as it is pulled away from the nucleus [Fig. 1(a)], mixing its ground state energy level with the higher orbital excited states [7]. Following the original proposal by Kane [4], several theoretical studies have examined Stark tuning of both donor electron and nuclear spins [7–10], while experiments have focused on measuring the Stark (or also strain-induced) shift parameters using electron spin resonance (ESR) of the donor [11–13]. These measurements showed a typical Stark-shift induced change in the hyperfine coupling on the order of kHz (for electric fields around 0.1 $\mathrm{V}/\mu\mathrm{m}$). This falls well within the ensemble ESR linewidth (12 MHz in natural silicon, or typically 100 kHz in silicon-28 limited by the magnetic field homogeneity), making it difficult to Stark shift the electron spin by more than a linewidth.

The nuclear spin, on the other hand, typically has much smaller spin resonance linewidth compared to the electron spin ($\gamma_n/\gamma_e = \sim 4 \times 10^{-4}$, where $\gamma_{n/e}$ is the gyromagnetic ratio of the nuclear/electron spin) and yet the effect of the Stark-tuned hyperfine shift on the nuclear spin resonance frequency is nearly the same as for the electron spin. As a consequence, using the Stark effect to tune nuclear spins in and out of resonance with globally applied fields becomes more readily achievable. Frequency shifts for both the electron and nuclear spins are expected to be typically below 1 MHz; i.e., Rabi oscillations will have to be even slower to achieve frequency selectivity between the in and out of resonance spins. This would limit electron spin manipulation time closer to that of the nuclear spin. Furthermore, the coherence time of the nuclear spin could reach minutes as measured in ensembles [14] (though currently limited to 20 ms in single spin devices [15]), potentially allowing a much larger number of Stark-shift-controlled quantum operations to be applied.

In this Letter, we examine the use of the Stark shift to conditionally manipulate the nuclear spin of antimony donors in silicon. We further demonstrate how the Stark shift can either be used as the basis for a simple controlled-phase gate or as a detuning gate to enable or disable the effect of a resonant magnetic radio frequency (rf) pulse. In the latter case, we are able to reach process fidelities above 90% by suppressing errors from electric field inhomogeneity. The techniques introduced here are directly applicable to numerous other spin systems that present coupling to electric field, be it either for the electron spin (with

 

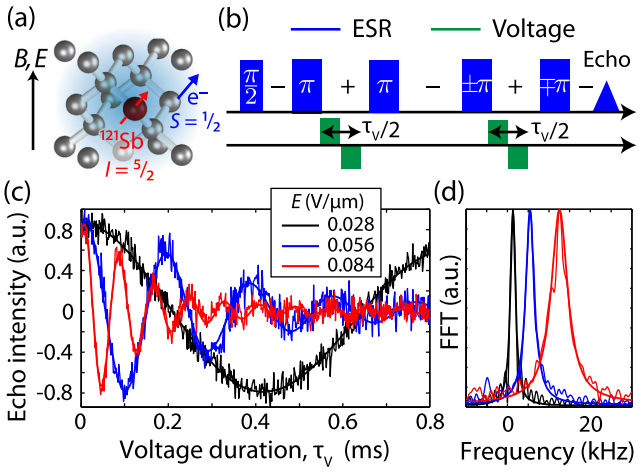


FIG. 1 (color online). Measurement of the Stark shift in $^{28}$Si:$^{121}$Sb using dynamical decoupling. (a) Cartoon of an antimony donor under the effect of an electric field. In light blue, the electron wave function is shifted from the donor nucleus. (b) Uhrig dynamical decoupling (UDD) sequence with four refocusing pulses. As each $\pi$ pulse reverses the phase acquisition (see signs in sequence), the dc electric field is applied in between alternating pairs of $\pi$ pulses. Using bipolar (positive and negative) voltage pulses, the linear Stark shift contribution is eliminated and only the quadratic part remains. The last two ESR pulses were phase cycled to remove any stimulated echoes. (c) Electron spin phase evolution measurement using the $m_I = -5/2$ ESR transition for different electric fields. (d) Fourier transform showing the frequency shift distribution in the sample with a Lorentzian fit.

crystal-field splitting such as NV centers [16]) or the nuclear spin (with hyperfine interaction such as rare earth doped crystal [17] or single molecule magnet [18]).

Measurements were conducted using an isotopically enriched silicon-28 float-zone crystal doped with antimony ($^{121}$Sb) at a concentration of $10^{14}$ cm$^{-3}$. Pulsed ESR and electron-nuclear double resonance (ENDOR) experiments were realized in a Bruker X-band (≈0.3 T, 9.7 GHz) Elexsys system. The sample, 1.71 mm in thickness, was inserted between two metal plates connected to a semirigid copper nickel coaxial cable to apply the voltage pulses (see Supplemental Material [19], S1), and sat in a continuous-flow helium cryostat at around 4.5 K. Voltage pulses up to 150 V, equivalent to 0.09 V/$\mu$m, were created with a low power high-voltage amplifier. The electric field was applied parallel to the static magnetic field and the [100] crystal orientation.

In order to measure the amplitude and distribution of the Stark shift in our system, we first confirm and then extend the measurements by Bradbury *et al.* [11] on the Sb donor electron spins. The Stark shift is measured as the electric sensitivity $\eta_A$ and $\eta_{g_e}$ of the hyperfine contact interaction $A$ and the electron $g$ factor $g_e$, respectively ($|\gamma_e| = g_e\mu_B$, with $\mu_B$ the Bohr magneton). Together, the application of an electric field $E$ results in a total frequency shift, for a particular electron or nuclear spin transition (see Ref. [19], S0 for further details on the donor Hamiltonian):

$$\Delta f(E) = \left[(\eta_A A) \times \frac{df}{dA} + (\eta_{g_e} g_e) \times \frac{df}{dg_e}\right] E^2. \quad (1)$$

The derivatives $df/dA$ and $df/dg_e$ are dependent on the static magnetic field, $B_0$, due to possible mixing between the electron and nuclear states, especially at low fields. In the high field limit, for an electron spin transition, $df/dA$ is equal to $m_I$ (the nuclear spin projection) and $df/dg_e$ is equal to $\mu_B B_0$, while for a nuclear spin transition, $df/dA$ is equal to $1/2$ and $df/dg_e$ is 0 (see Ref. [19], S0 for additional details).

The frequency response is quadratic in the electric field, owing to the tetrahedral symmetry at each donor site [7,10,21]. However, any perturbation from this high-symmetry site (e.g., arising from local strains or internal electric fields from trapped charges in the crystal) gives an additional, linear Stark shift component. The effect of this linear term can be suppressed by the application of alternating positive and negative voltage pulses as introduced by Bradbury *et al.* [11] and used here.

The Stark shift is measured in a Ramsey-type ESR experiment where the frequency shift $\Delta f(E)$ is acquired as a phase shift in the electron spin over time. In addition, refocusing pulses, such as used in a Hahn echo sequence, can significantly extend the acquisition time. The $T_2$ of the electron spin is 7 ms, limited by instantaneous diffusion [22,23], though additional magnetic field noise in our spectrometer reduces this time to about a millisecond. To circumvent the effect of magnetic field noise, we use the Uhrig dynamical decoupling (UDD) sequence [24], with voltage pulses applied between every other pair of decoupling microwave pulses [Fig. 1(b)].

The phase evolution of the electron spin is shown in Fig. 1(c) as a function of the duration of the voltage pulse for various voltage amplitudes. For unipolar voltage pulses, the echo decays within one period of oscillation (see Ref. [19], S2) because of the inhomogenous nature of the linear Stark shift component. The application of bipolar voltage pulses can be used to select only the quadratic Stark shift, yielding many phase oscillations, limited only by the effective electric field distribution in the sample. Inhomogeneities in the electric field are expected due to surface roughness and imperfect alignment of the metal plate on the sample; however, the Fourier transform of the signal [Fig. 1(d)] shows a Lorentzian distribution which is suggestive of a different mechanism. This could arise from impact ionization of donors from energetic free electrons under the electric field [25]. Finally, the Stark shift parameters for $^{28}$Si:$^{121}$Sb where measured to be $\eta_A = (-3.5 \pm 0.6) \times 10^{-3}$ $\mu$m$^2$/V$^2$, in good agreement with Ref. [11], while $\eta_{g_e}$ is below our measurement

sensitivity ($< 10^{-5}$ $\mu m^2/V^2$). At the magnetic fields used here ($\approx$0.3 T), the $g$-factor Stark shift is therefore negligible.

We now move on to examine the effect of the electric field on the Sb nuclear spin, beginning with an analogous experiment to that above to create a nuclear phase gate. Measurements of the Sb nuclear spin are realized using a Davies ENDOR sequence [Fig. 2(a)] which projects the nuclear spin population onto the electron spin [26,27]. Figures 2(a)–2(c) illustrate how combining the rf pulses with electric field control enables arbitrary $X$ and $Z$ rotations to be performed on the nuclear spin. This demonstrates that for specific values of the voltage pulse duration and amplitude, it is possible to enable or disable the effect of the applied rf pulses [Fig. 2(d)]: when the voltage-induced nuclear spin phase shift is equal to $\pi$, the total sequence is always equivalent to a $\pi$ rf pulse, independent of the rf duration $\tau_{rf}$. The conditional operation on the nuclear spin had a total duration of about 0.5 ms which remains quite long even compared to the nuclear spin coherence times. However, the applied electric field of 0.09 V/$\mu$m is still far from the ionization energy of $\gtrsim$1 V/$\mu$m for donors in silicon [8,28], so in principle the voltage pulse durations could be significantly reduced.

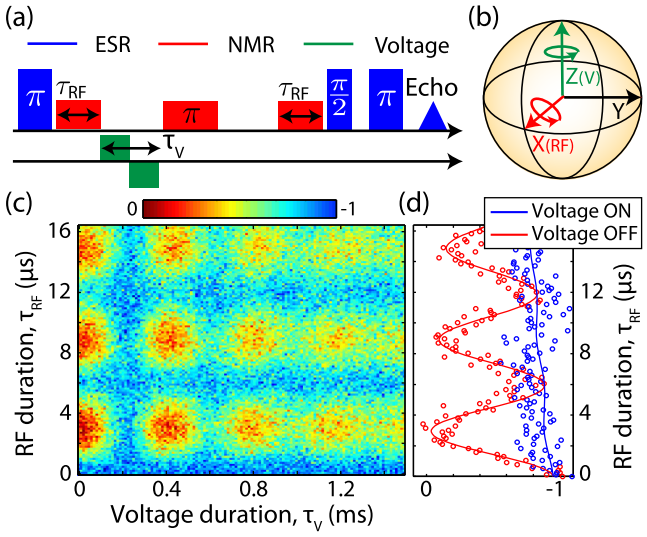


FIG. 2 (color online). Electrically controlled nuclear phase gate. (a) Measurement pulse sequence where a Hahn echo is used to refocus the inhomogeneous broadening happening during the application of the voltage pulse. (b) Bloch sphere representation of the nuclear spin rotations: in red, $X$ rotation from the rf pulse. In green, $Z$ rotation from the voltage pulse. (c) The duration of the voltage and rf pulses are independently swept in a 2D map, resulting in spin rotations about the $X$ and $Z$ axes. The measured electron spin echo intensity is $-1$ for an unperturbed nuclear spin, and 0 when the nuclear spin population is fully inverted, as is typical for Davies ENDOR measurements. (d) Projection of the 2D map for $\tau_V = 0$ ("off") and 0.2 ms ("on"), showing how the nuclear spin can be made effectively insensitive to the applied rf field for an appropriate duration of the (150 V) voltage pulse.

We next use, in Fig. 3, the electric field to tune the nuclear spin NMR frequency in or out of resonance with an applied rf field. At our maximum electric field ($< 0.1$ V/$\mu$m) and for the $m_I = \pm 5/2$ ESR transition, the frequency shift of 12 kHz cannot be resolved against the ESR linewidth of 50 kHz. For the nuclear spin (NMR transition) the frequency shift was measured to be 2.5 kHz (5 times lower than for the electron, as expected from the $m_I/m_S$ ratio), while the NMR linewidth is 500 Hz, 2 orders of magnitude smaller than for the electron (and partially limited by strain induced from the metal plates).

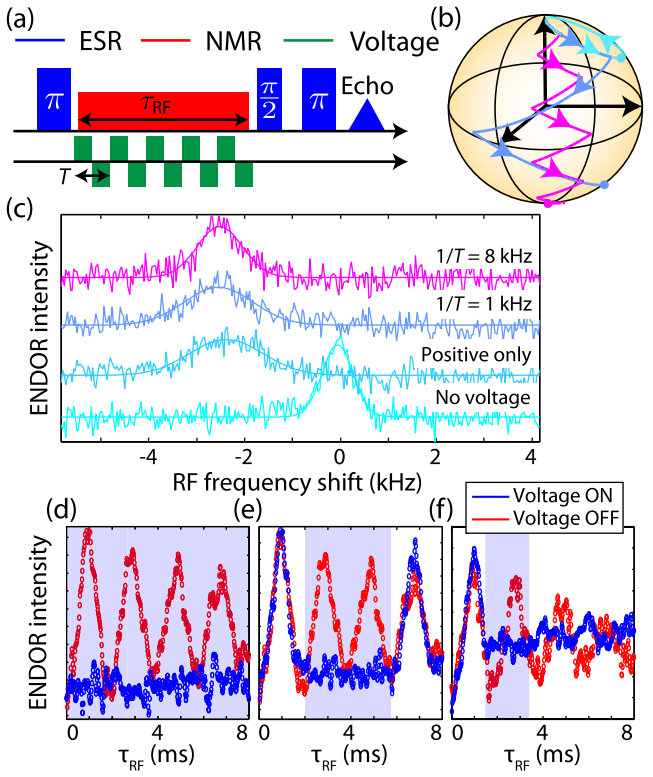


FIG. 3 (color online). Electrically tuning the nuclear spin transition frequency. (a) Davies ENDOR sequence with square wave voltage pulses. (b) Bloch sphere representation of the nuclear spin evolution in the rotating frame at the rf frequency which is resonant under a pure quadratic Stark shift. The linear Stark shift component adds additional off-resonant evolution, which can be compensated by applying a square-wave voltage pulse. (c) ENDOR spectra measured with and without 150 V pulses, where $\tau_{rf} = 1$ ms corresponding to a $\pi$ pulse. For a single unipolar voltage pulse, the shifted line is broadened by the linear Stark shift. The shifted ENDOR line can be narrowed by increasing the frequency of a square wave bipolar voltage pulse, up to a point, when it becomes limited by electric field inhomogeneity. (d)–(f) Nuclear spin Rabi oscillations, where: (d) the voltage is constantly applied; (e) the voltage is applied only within the light blue window which starts when the nuclear spin is in an eigenstate; (f) the voltage is applied within the light blue window which starts when the nuclear spin is in a coherent superposition state.

Figure 3(c) shows the ENDOR spectrum around the $m_S = +1/2$ nuclear spin transition, recorded for different voltage pulses. Applying a unipolar voltage pulse for the full duration of the rf pulse is sufficient to fully shift the NMR line by more than a linewidth; however, the linewidth broadens due to electric field inhomogeneity and, in particular, the linear Stark effect. The latter can be suppressed using a voltage pulse of alternating polarity, i.e., a square wave with a frequency faster than the spin evolution rate under the rf and voltage pulses (see calculations in Ref. [19], S4). This is shown in Figs. 3(a) and 3(b), allowing the Stark-shifted peak to narrow to a similar linewidth to the unshifted peak. The electric field inhomogeneity is not corrected with this sequence and as a result the peak linewidth and intensity cannot be fully recovered.

The ability to tune Sb nuclear spins in and out of resonance with an applied rf field is shown in Figs. 3(d)–3(f). When tuned off resonance by the Stark shift, the coherent rotation of the nuclear spins can be completely suppressed, or paused (voltage applied during the light blue window), for some given duration. This works effectively if the voltage pulse is applied when the nuclear spin is in an eigenstate [Figs. 3(d) and 3(e)]; however, when the nuclear spin is in a coherent superposition [Fig. 3(f)], rapid dephasing caused by the applied electric field leads to incomplete recovery of the nuclear spin state after the end of the voltage pulse. The electric field inhomogeneity results in a distribution in the phase acquired by each spin (leading to signal loss for the overall ensemble). Even without such inhomogeneity, one would need to keep track of the acquired phase while off resonant, which could become very complex for a large number of single qubits. To solve this problem, a hard $\pi$ refocusing rf pulse can be applied halfway through the rf rotation [Fig. 4(a)]. It has the same frequency as the other rf pulses but with a much higher bandwidth (shorter, higher power pulse) that excites the nuclear spin regardless of any Stark-shift detuning. Similar to a Hahn echo, any phase acquired during the first half of the voltage pulse is therefore refocused during the second half. As shown in Fig. 4(b), the recovered nuclear spin coherence now decays much more slowly.

With most of these source of errors suppressed, we finally evaluate the performance of the conditional nuclear spin gate using quantum process tomography [29–32] (see Ref. [19], S5). In the absence of an applied voltage pulse, the gate indeed acts as a $\pi_Y$ rotation with a process fidelity $F_{\text{proc}} = \text{Tr}(\chi_{\text{exp}}\chi_{\text{ideal}}) = 87.5\% \pm 6.4\%$, where $\chi_{\text{exp}}$ and $\chi_{\text{ideal}}$ are the measured and expected process matrices, respectively [Fig. 4(c)]. The fidelity is strongly reduced here by the inhomogeneous broadening of the nuclear spin ($T_{2n}^*$) as the slow rf pulse cancels the strong hard $\pi$ pulse. Under an applied voltage pulse, the total gate resembles the identity operation with a fidelity $F_{\text{proc}} = 93.3\% \pm 2.6\%$,

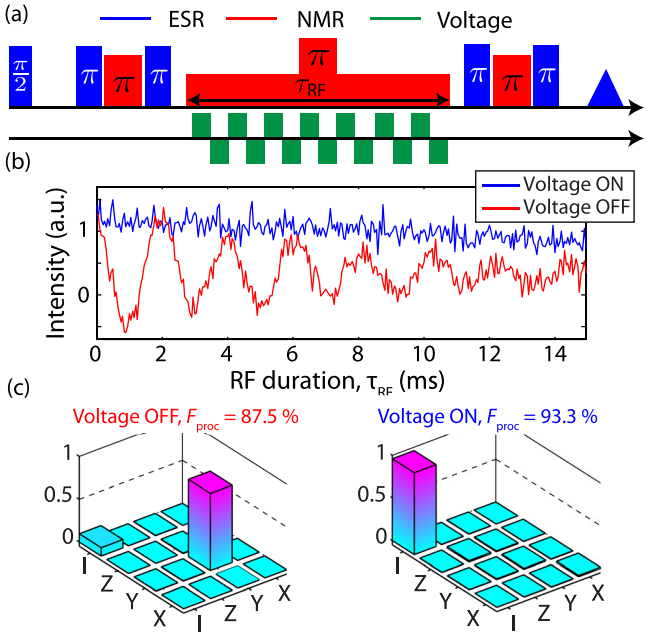


FIG. 4 (color online). (a) Sequence taken from Ref. [29] used for transferring an electron state to a nuclear state. This is used to produce any input state ($\pm X$, $\pm Y$, $\pm Z$ and identity) due to limited rf phase control in our experiment. The $\pi$ rf gate in the middle is a large bandwidth (≈30 kHz) and refocuses any dephasing when the voltage is on. (b) Rabi oscillations with and without voltages for an input coherent superposition. The oscillations decay quite fast for negative amplitudes as they correspond to even number of $\pi$ pulses which prevent refocusing of the nuclear coherence. (c) Quantum process tomography $\chi_{\text{exp}}$ matrices with voltage on (fidelity compared to a $Y$ rotation) and voltage off (fidelity compared to the identity matrix). Only the real part is shown as the imaginary part is negligible.

consistent with the upper theoretical limit of 94.1% estimated from the measured ENDOR linewidth and frequency shift (see Ref. [19], S5).

Strategies for further increasing the gate fidelities and overcoming effects such as electric field inhomogeneities include exploring composite pulses to address systematic errors [33], or the use of adiabatic sweeps to tune the spins through resonance during the microwave pulse [34,35]. These techniques could be rather insensitive to variations in the electric field and microwave, though at the expense of longer gate durations.

In conclusion, we have shown how the nuclear spin of a donor can be effectively controlled through a combination of rf excitation and an external electric field, either through electrically controlled phase gates or by detuning spins off resonance. The techniques we discuss for dealing with electric field inhomogeneities are not limited to ensembles of spins. They could be particularly useful when using electric fields to address a subset of spins in a device, such as tuning out a row of spins in an array. They could also reduce errors from slow temporal variations or crosstalk

between nearby qubit gates. Finally, by increasing the electric field closer to the onset of donor ionization, these conditional nuclear spin gates could have time scales of order 10 $\mu$s, which compares favorably to the minutes-long nuclear coherence times.

We thank C. C. Lo, R. Lo Nardo, A. M. Tyryshkin, and S. A. Lyon for valuable discussions and experimental help. This research is supported by the EPSRC through the Materials World Network (EP/I035536/2), the UNDEDD project (EP/K025945/1) and a DTA, as well as by the European Research Council under the European Community's Seventh Framework Programme (FP7/2007-2013)/ERC Grant Agreement No. 279781. J. J. L. M. is supported by the Royal Society. The $^{28}$Si-enriched samples used in this study were prepared from Avo28 material produced by the International Avogadro Coordination (IAC) Project (2004-2011) in cooperation among the BIPM, the INRIM (Italy), the IRMM (EU), the NMIA (Australia), the NMIJ (Japan), the NPL (UK), and the PTB (Germany).

*gary.wolfowicz@materials.ox.ac.uk
†jjl.morton@ucl.ac.uk

[1] S. Simmons, R. M. Brown, H. Riemann, N. V. Abrosimov, P. Becker, H.-J. Pohl, M. L. W. Thewalt, K. Itoh, and J. Morton, Nature (London) **470**, 69 (2011).
[2] J. J. Pla, K. Y. Tan, J. P. Dehollain, W. H. Lim, J. J. L. Morton, D. N. Jamieson, A. S. Dzurak, and A. Morello, Nature (London) **489**, 541 (2012).
[3] J. J. Pla, K. Y. Tan, J. P. Dehollain, W. H. Lim, J. J. L. Morton, F. A. Zwanenburg, D. N. Jamieson, A. S. Dzurak, and A. Morello, Nature (London) **496**, 334 (2013).
[4] B. E. Kane, Nature (London) **393**, 133 (1998).
[5] C. D. Hill, L. C. L. Hollenberg, A. G. Fowler, C. J. Wellard, A. D. Greentree, and H. S. Goan, Phys. Rev. B **72**, 045350 (2005).
[6] L. C. L. Hollenberg, A. D. Greentree, A. G. Fowler, and C. J. Wellard, Phys. Rev. B **74**, 045311 (2006).
[7] G. D. J. Smit, S. Rogge, J. Caro, and T. M. Klapwijk, Phys. Rev. B **70**, 035206 (2004).
[8] M. Friesen, Phys. Rev. Lett. **94**, 186403 (2005).
[9] R. Rahman, C. J. Wellard, F. R. Bradbury, M. Prada, J. H. Cole, G. Klimeck, and L. C. L. Hollenberg, Phys. Rev. Lett. **99**, 036403 (2007).
[10] R. Rahman, S. H. Park, T. B. Boykin, G. Klimeck, S. Rogge, and L. C. L. Hollenberg, Phys. Rev. B **80**, 155301 (2009).
[11] F. R. Bradbury, A. M. Tyryshkin, G. Sabouret, J. Bokor, T. Schenkel, and S. A. Lyon, Phys. Rev. Lett. **97**, 176404 (2006).
[12] L. Dreher, T. A. Hilker, A. Brandlmaier, S. T. B. Goennenwein, H. Huebl, M. Stutzmann, and M. S. Brandt, Phys. Rev. Lett. **106**, 037601 (2011).
[13] C. C. Lo, S. Simmons, R. Lo Nardo, C. D. Weis, A. M. Tyryshkin, J. Meijer, D. Rogalla, S. A. Lyon, J. Bokor, T. Schenkel, and J. J. L. Morton, Appl. Phys. Lett. **104**, 193502 (2014).
[14] M. Steger, K. Saeedi, M. L. W. Thewalt, J. J. L. Morton, H. Riemann, N. V. Abrosimov, P. Becker, and H.-J. Pohl, Science **336**, 1280 (2012).
[15] J. T. Muhonen, J. P. Dehollain, A. Laucht, F. E. Hudson, T. Sekiguchi, K. M. Itoh, D. N. Jamieson, J. C. McCallum, A. S. Dzurak, and A. Morello, arXiv:1402.7140.
[16] E. Van Oort and M. Glasbeek, Chem. Phys. Lett. **168**, 529 (1990).
[17] W. Mims and G. Mashur, Phys. Rev. B **5**, 3605 (1972).
[18] S. Thiele, F. Balestro, R. Ballou, S. Klyatskaya, M. Ruben, and W. Wernsdorfer, Science **344**, 1135 (2014).
[19] See Supplemental Material at http://link.aps.org/supplemental/10.1103/PhysRevLett.113.157601 for additional measurement and simulation (bipolar pulses, tomography) details, which includes Refs. [11,20,29,30,32].
[20] N. Hatano and M. Suzuki, in *Quantum Annealing Other Optim. Methods* (Springer, New York, 2005), Vol. 68, pp. 37–68.
[21] W. Kohn, Solid State Phys. **5**, 257 (1957).
[22] A. Schweiger and G. Jeschke, *Principles of Pulse Electron Paramagnetic Resonance* (Oxford University Press, Oxford, 2001).
[23] A. M. Tyryshkin, S. A. Lyon, A. V. Astashkin, and A. M. Raitsimring, Phys. Rev. B **68**, 193207 (2003).
[24] G. S. Uhrig, Phys. Rev. Lett. **98**, 100504 (2007).
[25] W. Kaiser and G. Wheatley, Phys. Rev. Lett. **3**, 334 (1959).
[26] E. R. Davies, Phys. Lett. **47A**, 1 (1974).
[27] A. M. Tyryshkin, J. J. L. Morton, A. Ardavan, and S. A. Lyon, J. Chem. Phys. **124**, 234508 (2006).
[28] S. Žurauskas and A. Dargys, Phys. Status Solidi **121**, 385 (1984).
[29] J. J. L. Morton, A. M. Tyryshkin, R. M. Brown, S. Shankar, B. W. Lovett, A. Ardavan, T. Schenkel, E. E. Haller, J. W. Ager, and S. A. Lyon, Nature (London) **455**, 1085 (2008).
[30] A. M. Childs, I. L. Chuang, and D. W. Leung, Phys. Rev. A **64**, 012314 (2001).
[31] M. Ježek, J. Fiurášek, and Z. Hradil, Phys. Rev. A **68**, 012305 (2003).
[32] J. L. O'Brien, G. J. Pryde, A. Gilchrist, D. F. V. James, N. K. Langford, T. C. Ralph, and A. G. White, Phys. Rev. Lett. **93**, 080502 (2004).
[33] S. Wimperis, J. Magn. Reson., Ser. A **109**, 221 (1994).
[34] A. Tannús and M. Garwood, NMR Biomed. **10**, 423 (1997).
[35] H. Wu, E. M. Gauger, R. E. George, M. Möttönen, H. Riemann, N. V. Abrosimov, P. Becker, H.-J. Pohl, K. M. Itoh, M. L. W. Thewalt, and J. J. L. Morton, Phys. Rev. A **87**, 032326 (2013).